Submitted to ApJ: 11 July 2004

A Neptune–Mass Planet Orbiting the Nearby M Dwarf GJ 436[1]

R. Paul Butler[2], Steven S. Vogt[3], Geoffrey W. Marcy[4], Debra A. Fischer[4,5], Jason T. Wright[4] Gregory W. Henry[6], Greg Laughlin[3] Jack J. Lissauer[7]

paul@dtm.ciw.edu

ABSTRACT

We report precise Doppler measurements of GJ 436 (M2.5V) obtained at Keck Observatory. The velocities reveal a planetary companion with orbital period of 2.644 d, eccentricity of 0.12 (consistent with zero) and velocity semi-amplitude of $K = 18.1$ m s^{-1} . The minimum mass ($M \sin i$) for the planet is 0.067 M_{JUP} = 1.2 M_{NEP} = 21 M_{EARTH}, making it the lowest mass exoplanet yet found around a main sequence star and the first candidate in the Neptune mass domain. GJ 436 (Mass = 0.41 $M_\odot$) is only the second M dwarf found to harbor a planet, joining the two–planet system around GJ 876. The low mass of the planet raises questions about its constitution, with possible compositions of primarily H and He gas, ice/rock, or rock–dominated. The implied semi–major axis is $a = 0.028$ AU = 14 stellar radii, raising issues of planet formation, migration, and tidal coupling with the star. GJ 436 is > 3 Gyr old, based on both kinematic and chromospheric diagnostics. The star exhibits no photometric variability on the 2.644-day Doppler period to a limiting amplitude of 0.0004 mag, supporting the planetary interpretation of the Doppler periodicity. Photometric

---

[1]Based on observations obtained at the W.M. Keck Observatory, which is operated jointly by the University of California and the California Institute of Technology. Keck time has been granted by both NASA and the University of California.

[2]Department of Terrestrial Magnetism, Carnegie Institution of Washington, 5241 Broad Branch Rd NW, Washington DC, USA 20015-1305

[3]UCO/Lick Observatory, University of California at Santa Cruz, Santa Cruz, CA, USA 95064

[4]Department of Astronomy, University of California, Berkeley, CA USA 94720

[5]Department of Physcis and Astronomy, San Francisco State University, San Francisco, CA, USA 94132

[6]Center of Excellence in Information Systems, Tennessee State University, 330 10th Avenue North, Nashville, TN 37203; Also Senior Research Associate, Department of Physics and Astronomy, Vanderbilt University, Nashville, TN 37235

[7]Space Science Division, 245-3 NASA Ames Research Center, Moffett Field, CA 94035-1000 USA

transits of the planet across the star are ruled out for gas giant compositions and are also unlikely for solid compositions. As the third closest known planetary system, GJ 436 warrants follow–up observations by high resolution optical and IR imaging and by the Space Interferometry Mission.

Subject headings: planetary systems – stars: individual (GJ 436, HIP 57087, LHS 310)

1. Introduction

To date, ∼135 extrasolar planets are securely known around nearby FGKM stars. All were discovered by the Doppler technique (see references within Butler et al. (2002) and Mayor and Santos (2003).[8]). The minimum masses span the range from 0.1 M_{JUP} to above 13 M_{JUP}, merging into the "brown dwarf" domain. The distribution of planet masses rises steeply toward the lowest detectable masses with a power law dependence, $dN/dM \propto M^{-1.3}$ (Marcy & Butler 2000; Marcy et al. 2004a), even after correction for the unknown orbital inclination (Jorissen, Mayor & Udry 2001). Two of the domains that remain relatively unexplored are the distribution of planet masses below 1 M_{SAT} and the occurrence of planets in general for low mass stars.

The distribution of masses of planets below that of Saturn remains poorly constrained because of the difficulty in their detection, demanding Doppler precision of 3 m s^{-1} or better. Prior to the discovery reported herein, eight known exoplanets had $M \sin i$ below 1 M_{SAT}, namely those orbiting HD 16141 and HD 46375 (Marcy et al. 2000), HD 16874 (Pepe et al. 2002), HD 76700 (Tinney et al. 2003), HD 49674 (Butler et al. 2003), HD 3651 (Fischer et al. 2003), 55 Cnc (planet "c", Marcy et al. 2002) and HD 99492 (Marcy et al. 2004b). HD 46375 and HD 99492 have the lowest known minimum masses, both having $M \sin i$ = 0.11 M_{JUP} = 0.3 M_{SAT} . Two sub–saturn candidates reside in distinctly eccentric orbits, namely HD 16141 (P=75 days, e=0.18) and HD 3651 (P=62.2 d, e = 0.64), suggesting that whatever mechanism pumps eccentricities in exoplanets, it acts on planets of sub–Saturn mass as well as on planets of ∼10 M_{JUP} .

Only one planetary system was previously known around an M dwarf, GJ 876 with its two planets (Marcy et al. 2001). The total number of M dwarfs being surveyed by precise Doppler measurements is roughly 200 (Wright et al. 2004, Mayor & Santos 2003, Kurster et al. 2003, Endl et al. 2003). The solitary planetary system (GJ 876) known around M dwarfs implies that the occurrence rate of planets having masses greater than 1 M_{JUP} and orbiting with periods, P < 3 yr (a < 1.5 AU), is only ∼0.5 %. In contrast, the occurrence rate of analogous planets around F & G–type main sequence stars is ∼5% (Mayor & Santos 2003; Marcy et al. 2004a) for such orbital periods. Thus, the occurrence rate of Jupiter–mass

[8]References to published papers and updates on orbital parameters can be found at http://exoplanets.org/

planets around M dwarfs having masses, M=0.3–0.5 $M_\odot$ is roughly an order of magnitude lower than that around F & G main sequence stars with M = 0.8–1.2 $M_\odot$.

Obviously, this approximate estimate of the occurrence of jupiters as a function of stellar mass suffers both from selection effects and from small numbers. The faintness of M dwarfs makes Doppler measurements more difficult. Nonetheless, planets of Jupiter–mass would make a Doppler signature of at least 20 m s^{-1} for orbits within 2 AU, rendering them easily detectable. Thus, the decline in planet occurrence with smaller stellar mass has statistical integrity, although the data are insufficient to establish an accurate relationship.

The diversity of planetary systems, including their observed masses and orbits, almost certainly stems from formation processes in protoplanetary disks (see for example, Lissauer 1995; Levison, Lissauer, & Duncan, 1998; Alibert, Mordasini, & Benz 2004). Young, low mass stars may be surrounded by protoplanetary disks that have lower mass and lower surface mass density than those surrounding young solar mass stars (T Tauri stars). If so, the formation of Jupiter–mass planets may be inhibited at all orbital radii (Laughlin, Bodenheimer, Adams 2004). Thus, low mass planets of Neptune–Saturn mass may be as common around M dwarfs as Jupiter–mass planets are around solar mass stars. Alternatively, gas accretion may operate so much less efficiently, or the lifetime of the gas may be so short, in low mass protoplanetary disks that predominantly rock–ice cores form only, with few gas giants forming.

More M dwarfs should be surveyed to establish the dependences of planet properties on stellar mass, especially at detection thresholds of sub–Saturn masses. Here, we report the detection of a planet with the lowest $M \sin i$ yet found, orbiting an M dwarf.

2. Properties of GJ 436

2.1. Mass and Age

GJ 436 (HIP 57087, LHS 310) is an M2.5V star with V = 10.67, B–V = 1.52 and a parallax of 97.73 mas (d = 10.23 pc) with an uncertainty of 3% from Hipparcos (ESA 1997) implying an absolute visual magnitude, M_V= 10.63, consistent with typical field M dwarfs of its spectral type residing on the main sequence.

Its mass may be estimated from various empirical mass–luminosity calibrations and theoretical models for M dwarfs. The empirical relation between stellar mass and M_V from Henry & McCarthy (1993) suggests that $M_\star = 0.42 \pm 0.05$ $M_\odot$, where the uncertainty stems from the standard deviation of the observed scatter in the stars of measured mass at a given M_V. Benedict et al. (2001) provide an updated mass–luminosity relation which agrees well with that from Henry & McCarthy. Delfosse et al. (2000) use their newly discovered M dwarf binaries, the calibration from which yields a mass for GJ 436 of 0.40 ± 0.05 $M_\odot$, in good agreement with that of Henry & McCarthy. Theoretical models from Baraffe et al. (1998) for solar metallicity, [M/H] = 0.0, predict a mass of 0.40 $M_\odot$ for GJ 436. Their

models suggest that if the star were metal–rich, [M/H] = +0.25, the implied mass would be higher by approximately 0.05 $M_\odot$, constituting a plausible systematic error due to the unknown metallicity of the star. The models of Siess et al. (2000) suggest a mass of 0.35 $M_\odot$, somewhat less than that from the empirical relation. Here we adopt the simple average of the two empirical estimates from Henry & McCarthy (1993) and from Delfosse et al. (2000) for GJ 436 yielding M=0.41 ± 0.05 $M_\odot$.

The age of GJ 436 may be constrained by various diagnostics. Leggett (1992) reports Galactic UVW velocities of +45.3, -20.0, +17.9 km s^{-1} , in agreement with Reid, Hawley, & Gizis (1995) who give +44, -20, +20. These velocities render the star a member of the "old disk" population. Indeed, for M dwarfs fainter than V = 10, there remains a kinematic bias toward identification of older, metal–poor stars and subsequent inclusion in catalogs (Reid, Hawley, Gizis 1995; Carney, Latham & Laird 1990). Its UVW velocity components suggest that GJ 436 has an age of at least 2 Gyr and probably has a metal abundance not much greater than solar. Furthermore, GJ 436 is not a flare star nor does it exhibit particularly strong chromospheric emission at Ca II H & K (Figure 1) for an M dwarf of its spectral type. It shows no emission at the Balmer lines in our high resolution spectra. This low chromospheric activity is consistent with a star middle-aged or older, placing the age likely greater than 3 Gyr consistent with the kinematics. We measured the rotational line broadening to be, $v \sin i < 3$ km s^{-1} (§5). Also, GJ 436 is photometrically constant at millimag levels (see §6), indicating that spots and magnetic fields are weak, consistent with an age greater than 3 Gyr.

2.2. Velocity Jitter and Ca II H&K

The photospheric velocity jitter of GJ 436 may be estimated from the ∼30 other M dwarfs on our Keck planet–search program that have similar stellar properties, namely B-V between 1.4 and 1.6, similar M_V, and similar Ca II H & K emission, as described by Wright et al. (2004), and have been observed at least 10 times over 4 or more years. In brief, the ∼ 30 M dwarfs of similar spectral type, M_V, and R'_{HK} are deemed comparison stars. For each of them the RMS of their velocity measurements is determined and the internal velocity error is subtracted in quadrature. The remaining velocity scatter represents the variance of our velocities caused by all sources excluding photon–limited errors. A minority of our comparison M dwarfs may have unseen companions which would raise the velocity RMS above that caused simply by photospheric jitter. Thus, Wright et al. determine the median value (instead of the mean) of those RMS values for the comparison stars, to suppress the effect of companions. The resulting median of the RMS values is found to be 3.3 m s^{-1}, with a standard deviation of 2.1 m s^{-1} about that median. This estimated jitter of 3.3 m s^{-1} is presumably due to convective overshoot, spots, flares, oscillations, and other non–uniformities on the rotating stellar surface. However, this jitter estimate, by its empirical construction, also includes errors caused by any instrumental and software inadequacies, as well as by low mass planets, that cause variations in our actual velocity measurements.

Endl et al. (2003) obtained 17 radial velocity measurements of GJ 436 using the Hobby–Eberly Telescope during 394 days. Those velocities exhibited an RMS of 20.6 m s^{-1}, constituting an excess velocity variability above errors. Their search for periodicities did not a reveal significant signal. Endl et al. (2003) considered carefully the possibility that jitter was the cause of the excess velocity scatter. They note that its stellar magnetic activity level and X–ray luminosity ($L_{\rm X} = 0.6 \times 10^{27} {\rm ergs - s^{-1}}$) are modest and similar to other quiet, old M dwarfs (such as GJ 411) that show a velocity RMS of less than 10 m s^{-1} , suggesting that the jitter of GJ 436 should be similarly smaller than 10 m s^{-1} . Our analysis similarly finds that GJ 436 is only modestly active, consistent with jitter of $\sim$ 3 m s^{-1}. Thus, it is quite possible that some of the excess velocity scatter noted by Endl et al. (2003) was caused by the planet we detect here. Our velocities (presented in Table 1) are not inconsistent with the results plotted for GL 436 in Figure 6 of Endl et al. within their error bars of 12–19 m s^{-1}.

The chromospheric emission at the Ca II K line in GJ 436 is shown in Figure 1 along with the same line in four comparison M dwarfs with similar B-V and V magnitude. We measure emission at both the Ca II H & K lines and find an average value from 2000 to 2004 of $S_{HK} =$ 0.726 for GJ 436 (Wright et al. 2004) on the Mount Wilson scale (Baliunas et al. 1995). The apparent strong emission in Figure 1 is deceptively striking because of the weak UV continua of low temperature dwarfs. Indeed, the ratio of Ca II H & K flux to the bolometric flux of the star is only $\log R'_{\rm HK} =$ -5.22 representative of the most chromospherically inactive stars. However, the precise values of $R'_{\rm HK}$ for M dwarfs remain difficult to measure and carry uncertainties of $\sim$ 20% due to the poor calibration of UV continuum fluxes as a function of B-V for such low mass stars (Wright et al. 2004).

In Figure 1 we show the Ca II K emission from GJ 436 and four comparison stars with similar B-V. For dwarf stars of spectral type $\sim$M2.5, a chromospheric Mt. Wilson S value of 0.5–1.3 is typical, showing that emission from the chromospheric gas at $\sim$10,000 K competes easily with the faint UV continuum of these cool dwarfs. The comparison stars have chromospheric emission bracketing that of GJ 436, rendering them useful comparison stars for estimating photospheric jitter and velocity errors. The velocity scatter of the comparison stars range from 2.32 and 4.65 m s^{-1} over the past 4 to 6 years, as shown in Figure 2. A total of 32 program stars are fainter then $V = 10$ with B-V between 1.4 and 1.6 and have at least 10 observations spanning 4 years. The median velocity RMS of these 32 stars is 6.7 m s^{-1}, including GJ 436 and other as yet unknown planet bearing stars. The four comparison stars shown in Figures 1 & 2, along with the other M1.5–M3 dwarfs of modest chromospheric activity on our planet–search program, show that the *combined* velocity jitter and velocity errors for these middle-aged M1.5 – M3 dwarfs having V $>$ 10, is $\sim$ 5 m s^{-1}.

3. Doppler–Shift Measurements

3.1. Stellar Sample and Doppler Technique

We have been monitoring the radial velocities of 150 M dwarfs at the Keck 1 telescope for the past 4 years. Most were drawn from the Hipparcos catalog (ESA 1997), with supporting stellar information taken from Reid, Hawley & Gizis (1995). The sample comprises a complete sample of isolated M dwarfs (separation greater than 2 arcsec from any companion) accessible to Keck within 9 pc that are brighter than V = 11. The magnitude threshold favors selection of early–type M dwarfs, M0–M5, causing exclusion of dwarfs later than M5. A few of the 150 M dwarfs are fainter than V = 11 and a few are farther than 9 pc. Our complete sample of M dwarfs has been monitored for the past 3 – 7 years and is listed by Wright et al. (2004). For M dwarfs having magnitudes, V = 8 – 12, the typical exposure times are 4–8 minutes yielding a S/N ratio per pixel in the spectra of 300–75, respectively. The resulting radial velocity measurements have an internal precision of 2–8 m s^{-1} , based on the agreement (uncertainty in the mean) of the $\sim$ 400 spectral intervals of 2 Å.

We measure Doppler shifts by placing an Iodine absorption cell (Marcy & Butler 1992) near the focal plane of the telescope centered on the optical axis, to superimpose iodine lines on the stellar spectrum, providing a wavelength calibration and proxy for the point spread function (PSF) of the spectrometer (Valenti et al. 1995). The temperature of the cell is controlled to 50.0 ± 0.1 C and the pyrex Iodine cell is sealed so that the column density of iodine remains constant (Butler et al. 1996). The Keck Iodine cell was not altered during the entire duration of the project, preserving the zero–point of the velocity measurements despite any changes to the optics of the HIRES spectrometer. The HIRES spectrometer is operated with a resolution R $\approx$ 70000 and wavelength range of 3700 – 6200 Å (Vogt et al. 1994) though only the region 4950 – 6000 Å (with iodine lines) was used in the Doppler analysis. The Doppler shifts from the spectra are determined with the spectral synthesis technique described by Butler et al. (1996).

Representative sets of velocity measurements for 4 stars with similar B–V and V magnitude are shown in Figure 2. These four stars bracket GJ 436 in both apparent brightness and chromospheric activity. The four comparison stars exhibit RMS velocity ranging from 2.32 to 4.65 m s^{-1}, representing the bottom line in the error budget, including errors from limited photons, any instrumental effects, Doppler analysis errors, and astrophysical jitter effects for such stars.

3.2. Velocities of GJ 436

We obtained 42 high resolution spectra of GJ 436 at the Keck 1 telescope with the HIRES echelle spectrometer (Vogt et al. 1994) during the 4.5–year period, Jan 2000 to July 2004 (JD = 2451552.1 – 2453196.8). The times of observation, velocities, and uncertainties are listed in Table 1. The exposure times were 8 – 10 minutes, yielding S/N $\approx$ 150 and

resulting in an uncertainty in the radial velocity of 4.4 m s^{-1} (median) per exposure. Starting on 29 July 2003 (JD = 2452849), we noticed an apparent periodicity of 2.64 d in our extant velocities. During the ensuing year of observations, as we tested the existence of the prospective planet, we usually obtained three consecutive exposures within a night to reduce the photon–limited errors by $\sqrt{3}$ to $\sim$ 3 m s^{-1}. We suspect that inadequacies in our current deconvolution algorithm result in another 2 m s^{-1} of stochastic error caused by accentuated noise in our deconvolved spectrum. Refinement of our deconvolution algorithm for M dwarfs is in progress.

Figure 3 shows the measured velocities vs. time for GJ 436, with each point representing the binned velocities in intervals of 2 hours for clarity. The internal velocity uncertainty was typically 4.4 m s^{-1}(median) as gauged from the uncertainty in the mean of the 400 spectral chunks separately analyzed in the Doppler analysis. This Doppler uncertainty is similar to that of the comparison M dwarfs of similar V magnitude (Figure 2). The recently obtained multiple exposures which were binned to final velocity measurements from 2003.9 to the present, have uncertainties of only $\sim$ 3–4 m s^{-1}, benefitting from the greater number of photons collected.

The velocities for GJ 436 exhibit an RMS of 13.3 m s^{-1}. This scatter is much greater than the internal errors of 4.7 m s^{-1} that stem from the uncertainty in the mean of the 400 spectral chunks that are separately analyzed for their Doppler shifts. The expected jitter is only 3.3 m s^{-1} based on comparable M dwarfs, as discussed in section 2.2. One may compute the probability that the scatter would be as large or larger than 13.3 m s^{-1} due to chance fluctuations of the known doppler errors and jitter, added in quadrature. We adopt here the quadrature sum of internal Doppler error for each measurement and the expected jitter of 3.3 m s^{-1}, as the effective noise. We fit a straight line to the velocities and examine the reduced χ^2 for the residuals, adopting this effective noise as the uncertainty per measurement in the calculation of χ^2. The resulting reduced $\sqrt{\chi^2_\nu} = 2.57$ which has a probability of occurrence by chance of less than 0.001. Thus the velocity scatter in GJ 436 is larger than can be understood by known sources of errors and photospheric jitter.

4. Orbital Analysis

A periodogram of the entire set of Keck velocities for GJ 436 is shown in Figure 4. A strong peak resides at a period of 2.643 d. The the false alarm probability associated with this peak is FAP $< 10^{-3}$ based on both the analytical assessment of the number of independent frequencies (Gilliland and Baliunas 1987) and by Monte Carlo realizations in which the velocities are scrambled and power spectra recomputed at the scrambled velocities. The window function produces peaks that surround the peak at 2.64 d, but they are not statistically significant.

We have fit the velocities for GJ 436 with a Keplerian model including a floating linear velocity trend, as shown in Figure 5. The fit yields an orbital period, $P = 2.6441$ d, velocity

semi-amplitude $K = 18.1 \pm 1.2$ m s^{-1}, and an eccentricity of $e = 0.12$. All orbital parameters are listed in Table 2. Adopting the stellar mass of 0.41 $M_\odot$ (§2.1) implies a minimum mass for the orbiting companion of $M \sin i = 0.067$ M_{JUP} and a semi-major axis of 0.0278 AU. The linear velocity trend has slope of 2.7 ± 1.5 m s^{-1} per year, implying the possible existence of a more distant companion, but still only marginally credible.

The uncertainties in Table 2 are based on Monte Carlo realizations of the data. The best–fit radial velocity curve is subtracted from the original velocities and the residuals are adopted as representative of the amplitude and distribution of velocity noise from all sources, including velocity errors and photospheric jitter. The residuals are permuted and added back to the best-fit radial velocity curve, leaving the times of observation the same. This approach yields many realizations of the set of velocity measurements of the best–fit planet, assuming that the noise distribution is as exhibited by the residuals. A Gaussian distribution of errors was not assumed (but such a simplification yields similar values for the uncertainties in the orbital parameters). Each realization was fit with a Keplerian model, allowing calculation of the standard deviation of each orbital parameter. These are adopted as the 1–σ uncertainties, as listed in Table 2. Note that these quoted uncertainties do not incorporate the uncertainty in the massof the star itself.

The Keplerian fit yields residuals with a standard deviation of 5.26 m s^{-1}, consistent with the expected errors and the RMS for the comparison M dwarfs (Figure 2). Similarly, the fit yields $\sqrt{\chi^2_\nu} = 1.00$, indicating that the Keplerian model from a single planet is adequate to explain the velocities. The eccentricity of 0.12 ± 0.06 is nearly consistent with a circular orbit. Tidal coupling is expected for such a close planet, with an especially short circularization time scale if the planet is partially solid.

We attempted fits to the velocities using the simplest model, notably one with an assumed circular orbit and no allowed velocity trend. Such models have only three free parameters and the best–fit circular orbit model is shown in Figure 6. The resulting best–fit circular orbit has $P = 2.644$ d, $K = 14.0$ m s^{-1}, and $M \sin i = 0.052$ M_{JUP}, implying a mass slightly smaller than that found in the eccentric–orbit model with a trend. The circular orbit model (no trend) yielded residuals with RMS = 6.8 m s^{-1} and $\sqrt{\chi^2_\nu} = 1.25$, both somewhat larger than those found from the eccentric model, but not a large enough difference to rule it out. We then fit the velocities with a Keplerian having non–zero eccentricity, but no trend, which yielded $\chi^2_\nu = 1.20$ and $e = 0.11$. Finally, we fit the velocities with a circular orbit, but leaving the trend floating, which yielded RMS = 6.19 m s^{-1} and $\chi^2_\nu = 1.15$, and gave $M \sin i = 0.052$ M_{JUP}. This model consisting of a circular orbit with floating trend reduces χ^2_ν to a level that is near enough that achieved with the eccentricity allowed to float that we cannot rule out a circular orbit. Thus, a circular orbit remains plausible and implies a lower planet mass, $M \sin i = 16.5$ M_{Earth}.

5. False Alarm Probability

The Keplerian fit to the velocities yields an acceptable value of $\chi^2_\nu = 1.03$ when including a velocity trend, and yields nearly as acceptable a value, $\chi^2_\nu = 1.23$, when carrying out a fit with only a circular orbit and no trend. Nonetheless, one might be concerned that the plethora of possible orbits of short periods, less than ∼10 d, might permit random fluctuations to yield such low values of χ^2 by chance.

We tested the hypothesis that the velocities are merely uncorrelated noise such that the Keplerian fit yields a low χ^2 due merely to fluctuations of that noise. We have carried out two tests of this null hypothesis, one using the F–statistic and the other with Monte Carlo simulations of scrambled velocities. The F–Test is described by Ford (2004), Cumming (2004) and Marcy et al. (2004b). The improvement in χ^2 between a model that assumes no planet and one that includes a Keplerian orbit, $\Delta\chi^2$, can be assessed for the probability that such improvement would occur by chance fluctuations. We form the ratio $\Delta\chi^2/\chi^2_\nu$ which follows the F distribution (Bevington & Robinson 2002, Cumming 2004) and permits assessment of the probability that this ratio departs from 0.0 due to fluctuations alone. That probability corresponds to the false alarm probability (FAP) for the best–fit Keplerian model. Each independent frequency (1 / orbital period) can harbor such fluctuations. We therefore determine the number of independent frequencies (periods) by constructing an interval between them such that a phase difference of one full cycle accrues during the entire time series (Cumming 2004). This F–Test is essentially identical to the computation of FAP from a periodogram analysis. In our test, however, a Keplerian model, rather than a sinusoid, is compared to the no–planet model. We applied this test to GJ 436. We find that the probability that χ^2_ν improved due to mere fluctuations of noise from 2.57 (no planet) to 1.03 (Keplerian plus trend) is less than 1×10^{-5}. We thus find it unlikely that noise fluctuations can account for the low χ^2_ν found from the Keplerian model.

The F–Test cannot properly account for the non–uniform sampling of the velocities nor the non–Gaussian nature of the velocity errors. Therefore, we have carried out another test of FAP that involves scrambling the velocities, as if they were uncorrelated noise, and recomputing a Keplerian fit for each scrambled realization of the data. In this way, we determine the distribution of χ^2 that is expected if the velocities were simply uncorrelated noise.

We scrambled the velocities, keeping the times of observation the same. For each of 1000 realizations, we searched for the best–fit Keplerian model and recorded its associated value of χ^2. The resulting histogram of $\sqrt{\chi^2_\nu}$ is shown in Figure 7 and shows the distribution expected if the measured velocities were simply uncorrelated noise. The distribution peaks at $\sqrt{\chi^2_\nu} = 2.05$ with a width, FWHM = 0.3. None of the 1000 trials of scrambled velocities yielded a value of $\sqrt{\chi^2_\nu}$ below the best–fit $\sqrt{\chi^2_\nu}$ of 1.03 from the original velocities. Thus, if the measured velocities are simply noise, the probability is <1/1000 that the value of χ^2_ν for the best–fit Keplerian orbit planet would be caused by chance fluctuations. Moreover the distribution of $\sqrt{\chi^2_\nu}$ from scrambled velocities is so well separated from the value of $\sqrt{\chi^2_\nu}$ from the original velocities (Figure 7), that the FAP is likely to be significantly less than

0.001, consistent with the even lower FAP value found from the F–Test. This robust Monte Carlo analysis suggests directly that fluctuations in uncorrelated noise cannot account for the low χ^2 from the Keplerian fit. With a stellar sample of 150 M dwarfs on the Keck planet search, the probability is low that such chance fluctuations might arise in any one of the M dwarfs. Thus, the velocities appear inconsistent with the hypothesis that the high quality of the Keplerian fit stems merely from chance fluctuations.

We also considered that systematic errors might account for the velocity variations seen in GJ 436. We have computed periodograms from our velocity measurements of the other 150 M dwarfs obtained with HIRES during the past four years. None shows a periodicity anywhere near a period of 2.6 d with any amplitude close to the 18 m s^{-1} seen here. Thus, we see no evidence of any instrumental source of a 2.6–day periodicity. For the same reason, no other M dwarfs reveal any evidence of intrinsic *astrophysical* periodicities at that period. Similarly, the other 1100 FGK stars on our Keck planet–search program show no evidence of 2.6–day periodicities. Indeed, the shortest period planet found on this program is that of HD 46375 with a period of 3.02 d, rendering the 2.6–day period of GJ 436 clearly extraordinary in our Doppler planet survey.

One conceivable source of periodicity is the rotation of the star that could modify the spectrum due to any inhomogeneities on the stellar surface. However, we see no photometric periodicity in GJ 436 at periods near 2.64 d (Figure 8) at millimag levels. This lack of brightness variations suggests the absence of large spots and active regions distributed non–uniformly over the photosphere, with limits on the covering factor of under 1% . The star clearly has a chromosphere, as seen in the Ca II H & K emission (Figure 1), which is likely distributed in patches over magnetic regions. However, the Doppler information in optical spectra comes from the photosphere which apparently has uniform surface brightness, with fluctuations no more than 1% judging from the constant photometry.

If the 2.644–day Doppler period were the rotation period of star, the implied equatorial velocity would be 7.3 km s^{-1} (by adopting a stellar radius of 0.38 $R_\odot$) (Chabrier & Baraffe 2000). Such a large equatorial velocity could be detectable in the rotational broadening of the absorption lines. We compared the widths of the lines in GJ 436 to those in a comparison star, GJ 411 which has $V \sin i < 2$ km s^{-1} (Chen and Marcy 1992). We find that the lines in GJ 436 are no broader than those in GJ 411, giving an upper limit of 3 km s^{-1} on $V \sin i$. Thus the hypothesis that GJ 436 is rotating at nearly 7.3 km s^{-1} appears to be unlikely. Stellar rotation seems unlikely to be the cause of the Doppler periodicity at $P = 2.644$ d.

6. Photometric Observations

Queloz et al. (2001) and Paulson et al. (2004) have shown that photospheric features such as spots and plages on solar-type stars can result in low-amplitude, periodic radial velocity variations capable of mimicing the presence of a planetary companion. Therefore, precision photometric measurements are an important complement to Doppler observations

and can help to establish whether the radial velocity variations are caused by stellar magnetic activity or planetary-reflex motion, e.g., Henry et al. (2000a). Photometric observations can also detect possible transits of the planetary companions and so allow the determination of their radii and true masses, e.g., Henry et al.(2000b).

We have observed GJ 436 with the T12 0.8 m automatic photometric telescope (APT) at Fairborn Observatory between 2003 November and 2004 June and obtained a total of 226 brightness measurements. The T12 APT is equipped with a two-channel precision photometer employing two EMI 9124QB bi-alkali photomultiplier tubes to make simultaneous measurements in the Strömgren b and y passbands. The APT measures the difference in brightness between a program star and a nearby constant comparison star with a typical precision of 0.0015 mag for bright stars ($V < 8.0$). For GJ 436, we used the comparison star HD 102555 ($V = 7.24$, $B - V = 0.39$, F2), which was shown to be constant to 0.002 mag or better by comparison with the second comparison star HD 103676 ($V = 6.79$, $B - V = 0.38$, F2). We reduced our Strömgren b and y differential magnitudes with nightly extinction coefficients and transformed them to the Strömgren system with yearly mean transformation coefficients. Further information on the telescope, photometer, observing procedures, and data reduction techniques employed with the T12 APT can be found in Henry (1999) and in Eaton, Henry, & Fekel (2003).

The 226 combined $(b + y)/2$ differential magnitudes of GJ 436 are plotted in the top panel of Figure 8. The observations are phased with the planetary orbital period and a time of inferior conjunction, computed from the orbital elements in Table 2. The standard deviation of the observations from the mean brightness level is 0.0043 mag, larger than the typical 0.0015 mag precision with the T12 APT, because GJ 436, at $V = 10.67$, is much fainter than the typical star observed with this telescope. By averaging the Strömgren b and y observations into a single passband, we gained a factor of square root 2 in our precision, improving our sensitivity to any intrinsic stellar variability. Period analysis does not reveal any periodicity between 1 and 100 days. A least-squares sine fit of the observations phased to the radial velocity period gives a semi-amplitude of 0.00044 ± 0.00037 mag. Thus starspots are unlikely to be the cause of the velocity periodicity. If the star were pulsating with a velocity amplitude of 18 m s^{-1}, the difference between its minimum and maximum radius would be 1300 km, yielding a fractional change in disk size of 0.005. Thus, the observed very low limit to possible photometric variability supports planetary-reflex motion as the cause of the radial velocity variations. Note that even if the planet were as large as Jupiter, it would intercept only $3{\times}10^{-4}$ of the star's radiation.

The observations near phase 0.0 are replotted with an expanded abscissa in the bottom panel of Figure 8. The solid curve in each of the two panels approximates the predicted transit light curve assuming a planetary orbital inclination of 90° (central transits). The out-of-transit light level corresponds to the mean brightness of the observations. The transit duration is calculated from the orbital elements. Four different transit depths are estimated from an assumed stellar radius of 0.41 $R_\odot$, a planetary mass of 1.2 M_{NEP}, and planetary radii of 0.5, 0.35, 0.31, and 0.24 R_{JUP}, corresponding to planetary models of a gas giant without a core, a gas giant with a core, an ice/rock planet, and a planet composed of pure

iron, respectively. The horizontal bar below the predicted transit window in the bottom panel represents the approximate uncertainty in the time of mid transit, based on Monte Carlo simulations and the uncertainties in the orbital elements. The vertical error bar to the right of the transit window corresponds to the ± 0.0043 mag measurement uncertainties for a single observation. The geometric probablility of transits is 6.8%, computed from equation 1 of Seagroves et al. (2003) assuming random orbital inclinations. The mean of the 8 observations within the transit window agrees with the mean of the 218 observations outside the window to within 0.0010 mag, just as expected from the precision of the observations. Thus, central transits for the four planetary models given above would produce transit depths of 17, 8, 7, and 4 sigma, respectively. Although the uncertainty in the time of mid transit is somewhat larger than the duration of possible transits, the observations nonetheless rule out the possibility of complete (as opposed to grazing) transits except possibly for shallow events occuring around phase 0.99 for a planet with a rocky or iron composition. Since the planet lies at a distance of 14 stellar radii, the inclination of the orbit must be less than about 86°.

7. Discussion

The radial velocities of GJ 436 exhibit a marked periodicity, consistent with a Keplerian orbit of a planetary-mass companion. No other interpretation, such as stellar oscillations or rotational modulation of surface inhomogeneities, seems likely to explain the 2.6 d periodicity. The implied Keplerian orbit has a period of 2.644 d, an orbital semimajor axis of 0.0278 AU, and an orbital eccentricity of 0.12 that is marginally consistent with circular.

The stellar mass of 0.41 $M_\odot$ implies a minimum planet mass, $M \sin i$, of 0.067 M_{JUP} or 1.2 M_{NEP} . This minimum mass is considerably lower than that of any extrasolar planet previously found (pulsar planets aside). The lowest previously found planet, as of this writing, had been that of HD 49674 with $M \sin i = 0.11$ M_{JUP} (Butler et al. 2003). For randomly oriented orbits, the average value of $\sin i$ is $\pi/4$ and it is probable that $\sin i > 0.5$. Thus it is likely that this planet has a mass less than 2 M_{NEP}.

A planet of roughly Neptune mass orbiting 0.028 AU from an M dwarf raises several new issues about its constitution. We could not rule out the possibility of a solid rock or rock–ice composition, nor a primarily ice–rock body with a significant hydrogen envolope reminiscent of Neptune and Uranus in our Solar System. Indeed, one wonders if a gaseous envelope can be ruled out for this planet on the basis of its survival against UV energy deposition from the young, magnetic M dwarf. The uncertainty in its composition leaves a range of plausible radii for the planet, from 0.2 – 1.0 R_{JUP}(especially for arbitrary orbital inclinations), leaving uncertain the amount of dimming expected by transits. The planet intercepts 3×10^{-4} of the star's radiation, if it has the radius of Jupiter. This would be the amplitude of reflected light variations if the planet's albedo were unity and the orbit were edge–on.

After submission of this paper, another Neptune-mass planet ($M \sin i = 0.82$ M_{NEP})

emerged from Doppler measurements made by the Hobby Eberly Telescope and Lick Observatory (McArthur et al. 2004). Orbiting 55 Cancri (G8 V), this other neptune raises similar questions about its origin, migration, and composition. The existence of two planets having $M \sin i$ near the mass of Neptune drastically reduces the already remote statistical possibility that face–on orbital inclinations explain the low values of $M \sin i$ for them . Instead, it is likely that a population of Neptune–mass planets exists that is the extension of the rising mass function already known toward lower planetary masses.

From its M_V of 10.63 and expected bolometric correction of –1.9, the luminosity of GJ 436 is $L = 0.025$ L$_\odot$. At its orbital distance of 0.028 AU, the expected surface temperature is ~ 620 K, depending on its albedo, greenhouse effects, and uniform illumination, all of which are questionable. Most metals and refractory material remain solid at such a temperature which is similar to that on the surface of Venus. Insignificant mass loss would occur from the tail of the Maxwell–Boltzmann distribution of hydrogen. However, a detailed calculation is required to determine the mass loss from the planet due to high–energy stellar radiation from flares and the corona, especially during first billion years of enhanced magnetic activity on the star. The possibility of Roche–lobe overflow (in either direction) especially during pre–main–sequence evolution, should also be considered. Tidal coupling must be computed to determine if the planet keeps one hemisphere toward the star. If the planet were mostly solid, questions would be raised about the temperature on both the back side and on the terminator.

This star is just the second M dwarf known to harbor a planet, the first being two–planet system around GJ 876 (Marcy et al. 2001). At a distance of 10.2 pc, GJ 436 is a prime target for the Space Interferometry Mission (SIM) to detect the astrometric wobble and place limits on $\sin i$ and hence the planet mass. Coronagraphic imaging missions from the ground and space should attempt to image planets residing farther from this star, especially because of the velocity trend that seems to be preferred in our model.

We find that giant planets are rare among M dwarfs. Among the 150 M dwarfs in our Keck survey, this star is only the second found to have a planet despite three years of surveying them with high Doppler precision of 3 m s^{-1}. The low mass of this new planet highlights our ability to detect planets of somewhat higher mass, 0.3 M$_{\rm JUP}$ or greater within 1 AU ($P < 1.5$ yr) during which time at least two orbits would have transpired. However, only one M dwarf has revealed such a jupiter–sized planet around an M dwarf. Thus, the occurrence rate of Jupiter–mass planets within 1 AU of M dwarfs appears to be $1/150 \approx 0.7\%$. In contrast, among our 1180 FGK stars surveyed at the Lick, Keck, and AAT telescopes, 41 have a planet within 1 AU. Thus, for nearby FGK stars, the occurrence rate of jupiter–mass planets ($0.5 < M < 13$ M$_{\rm JUP}$) within 1 AU is 3.5% (Marcy et al. 2004a). Thus, the occurrence of jupiters orbiting near M dwarfs appears to be a factor of ~ 5 below that of solar–mass stars.

This paucity of giant planets around M dwarfs is consistent with, but not required by, the planet–formation models of Levison, Lissauer, & Duncan (1998) and of Alibert, Mordasini, & Benz (2004). Lower mass protoplanetary disks around M dwarfs may have

been important in slowing the accretion rate, yielding lower–mass planets (Laughlin et al. 2004). Indeed, the formation of Neptune in our Solar System is not well understood and may have been influenced by the low surface mass density in the outer Solar nebula (Lissauer et al. 1995; Bryden, Lin, & Ida 2000; Thommes, Duncan, & Levison 2002). Thus, it appears that the occurrence of jupiters is a function of stellar mass. Stars more massive than the Sun may harbor Jupiter-mass planets in greater numbers and masses than found so far around Solar–type stars.

We thank John Johnson, and Chris McCarthy for help with the observations and analysis, and we thank Eugene Chiang and Peter Bodenheimer for valuable conversations. We gratefully acknowledge the superb dedication and support of the Keck Observatory staff. We appreciate support by NASA grant NAG5-75005 and by NSF grant AST-0307493 (to SSV); support by NSF grant AST-9988087, by NASA grant NAG5-12182 and travel support from the Carnegie Institution of Washington (to RPB). GWH acknowledges support from NASA grant NCC5-511 and NSF grant HRD-9706268. JJL acknowledges support from NASA's Solar Systems Origins grant 188-07-1L. We are also grateful for support by Sun Microsystems. We thank NASA and the University of California for allocations of Keck telescope time toward the planet search around M dwarfs. This research has made use of the Simbad database, operated at CDS, Strasbourg, France. Finally, the authors wish to extend thanks to those of Hawaiian ancestry on whose sacred mountain of Mauna Kea we are privileged to be guests. Without their generous hospitality, the Keck observations presented herein would not have been possible.

REFERENCES

Alibert, Y., Mordisini, C. & Benz,W. 2004, A&A, 417, L25

Baliunas, S. L., et al. 1995, ApJ, 438, 269

Baraffe, I., Chabrier, G., Allard, F., Hauschildt, P. H. 1998, A&A, 337, 403

Benedict, G. F., McArthur, B. E., Franz, O. G., Wasserman, L. H., Henry, T. J., Takato, T., Strateva, I. V., Crawford, J. L., Ianna, P. A., McCarthy, D. W., Nelan, E., Jefferys, W. H., van Altena, W., Shelus, P. J., Hemenway, P. D, Duncombe, R. L., Story, D., Whipple, A. L., Bradley, A. J., Fredrick, L. W. 2001, AJ, 121, 1607

Bevington, P.& Robinson, K. D. 2002, "Data Reduction and Error Analysis for the Physical Sciences", McGraw–Hill Education

Chabrier, G & Baraffe, I. 2000, ARA&A, 38, 337

Bryden, G., Lin, D. N. C. & Ida , S. 2000, ApJ, 544, 481

Butler, R. P., Marcy, G. W., Williams, E., McCarthy, C., Dosanjh, P., & Vogt, S. S. 1996, PASP, 108, 500

Butler, R. P., Marcy, G. W., Vogt, S. S., Tinney, C. G., Jones, H. R. A., McCarthy, C., Penny, A. J., Apps, K., Carter, B. D., 2002 ApJ, 578, 565

Butler, R. P., Marcy, G. W., Vogt, S. S., Fischer, D. A., Henry, G. W., Laughlin, G. P., Wright, J. T. 2003, ApJ, 582, 455

Carney, B. W., Latham, D. W. & Laird, J. B. 1990, AJ, 99, 572

Chen, G. H. & Marcy, G. W. 1992, ApJ, 390, 550

Cumming, A. 2004, MNRAS, submitted.

Delfosse, X., Forveille, T., Ségransan, D., Beuzit, J.-L., Udry, S., Perrier, C., Mayor, M. 2000, A&A, 364, 217

Eaton, J. A., Henry, G. W., & Fekel, F. C. 2003, in The Future of Small Telescopes in the New Millennium, Volume II - The Telescopes We Use, ed. T. D. Oswalt (Dordrecht: Kluwer), 189

Endl, M., Cochran, W. D., Tull, R. G. & MacQueen, P. J. 2003, AJ, 126, 3099

ESA 1997, The Hipparcos and Tycho Catalogs, ESA-SP 1200

Fischer, D. A., Butler, R. P., Marcy, G. W., Vogt, S. S., & Henry, G. W. 2003, ApJ, 590, 1081

Ford, E. B. 2004, ApJ in press

Gilliland, R. L., & Baliunas, S. L. 1987 ApJ, 314, 766

Henry, G. W. 1999, PASP, 111, 845

Henry, G. W., Baliunas, S. L., Donahue, R. A., Fekel, F. C., & Soon, W. 2000a, ApJ, 531, 415

Henry, G. W., Marcy, G. W., Butler, R. P., & Vogt, S. S. 2000b, ApJ, 529, L41

Henry, T. J. & McCarthy, D. W., Jr. 1993, AJ, 106, 773

Jorissen, A., Mayor, M., & Udry, S. 2001, A&A, 379, 992

Kürster, M., Endl, M., Rouesnel, F., Els, S., Kaufer, A., Brillant, S., Hatzes, A. P., Saar, S. H.& Cochran, W. D., 2003, A&A, 403, 1077.

Laughlin, G. P., Bodenheimer, P., Adams, F 2004, submitted to Nature, "Core–Accretion Model Predicts Few Jovian Planets Orbiting Red Dwarfs"

Leggett, S.K. 1992, ApJS, 82, 351.

Levison, H., Lissauer, J. J. & Duncan, M. J. 1998, AJ, 116, 1998

Lissauer, J.J., 1995. Urey Prize Lecture: On the Diversity of Plausible Planetary Systems. Icarus 114, 217.

Lissauer, J.J., J.B. Pollack, G.W. Wetherill, and D.J. Stevenson 1995. Formation of the Neptune System. Neptune and Triton, D.P. Cruikshank, ed. (Tucson: University of Arizona Press), 37-108.

Marcy, G. W., & Butler, R. P. 1992, PASP, 104, 270

Marcy, G. W., & Butler, R. P. 2000, PASP, 112, 137

Marcy, G. W., Butler, R. P., & Vogt, S. S. 2000, ApJ, 536, L43–L46

Marcy, G. W., Butler, R. P., Fischer, D. A., Vogt, S. S., Lissauer, J. J., Rivera, E. J. 2001, ApJ, 556, 296

Marcy, G. W., Butler, R. P., Fischer, D. A., Laughlin, G., Vogt, S. S., Henry, G. W., & Pourbaix, D. 2002, ApJ, 581, 1375

Marcy, G. W., Butler, R. P., Fischer, D. A., & Vogt, S. S. 2004a, to appear in ASP Conf. Ser. 3xx: Extrasolar Planets, Today and Tomorrow", Ed. J.P. Beaulieu, A. Lecavelier & C.Terquem.

Marcy, G. W., Butler, R. P., Vogt, S. S.,Fischer, D. A., Henry, G. W., Laughlin, G., Wright, Jason, T., Johnson, J 2004b, Submitted to ApJ, "Six New Extrasolar Planets".

Mayor, M., & Santos, N. C. 2003, In Astronomy, Cosmology and Fundamental Physics, p. 359

McArthur, B. E., Endl, M., Cochran, W. D., Benedict, G. F., Fischer, D.A., Marcy, G. W., Butler, R. Paul, Naef, D., Mayor, M., Queloz, D., Udry, S. & Harrison, T. E. 2004, Submitted to ApJ Letters.

Paulson, D. B., Saar, S. H., Cochran, W. D., & Henry, G. W. 2004, ApJ, 127, 1644

Pepe, F., Mayor, M., Galland, F., Naef, D., Queloz, D., Santos, N. C., Udry, S., Burnet, M. 2002, A&A, 388, 632

Queloz, D., Henry, G. W., Sivan, J. P., Baliunas, S. L., Beuzit, J. L., Donahue, R. A., Mayor, M., Naef, D., Perrier, C., & Udry, S. 2001, A&A, 379, 279

Reid, I. N., Hawley, S. L., Gizis, J. E. 1995, AJ, 110,1838.

Seagroves, S., Harker, J., Laughlin, G., Lacy, J., & Castellano, T. 2003, PASP, 115, 1355

Siess, L., Dufour, E., Forestini, M. 2000, A&A, 358, 593

Thommes, E. W., Duncan, M. J., Levison, H. F. 2002, AJ, 123 2862

Tinney, C. C., Butler, R. P., Marcy, G. W., Jones, H. R. A., Penny, A. J., McCarthy, C., Carter, B., Bond, J. 2003, ApJ, 587, 423

Valenti, J. A., Butler, R. P.,& Marcy, G. W 1995, 107, 966

Vogt, S. S. et al. 1994. Proc. Soc. Photo-Opt. Instr. Eng., 2198, 362.

Wright, J. T., Marcy, G. W., Butler, R. P., Vogt,S.S. 2004, ApJS, 152, 261

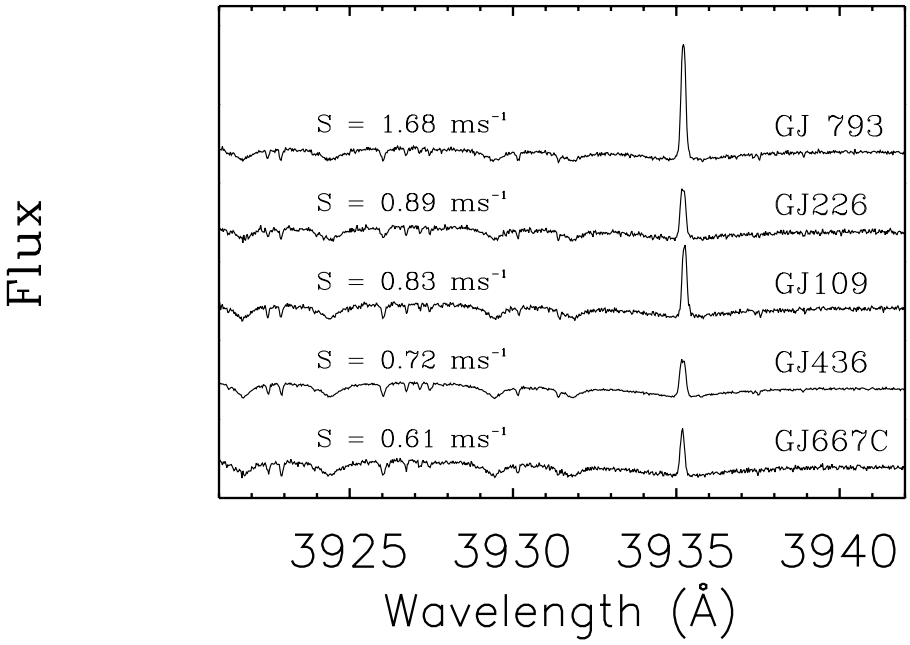

Fig. 1.— Spectra of the chromospheric Ca II K emission line for GJ 436 and four comparison M dwarfs with the similar B-V and V magnitude. The stars are plotted in the ascending order of chromospheric S value: GJ 667C (*bottom*), GJ 436, GJ 109, GJ 226, and GJ 793 (*top*). These four comparison stars have chromospheric emission that bracket that of GJ 436, rendering them good comparison stars for GJ 436.

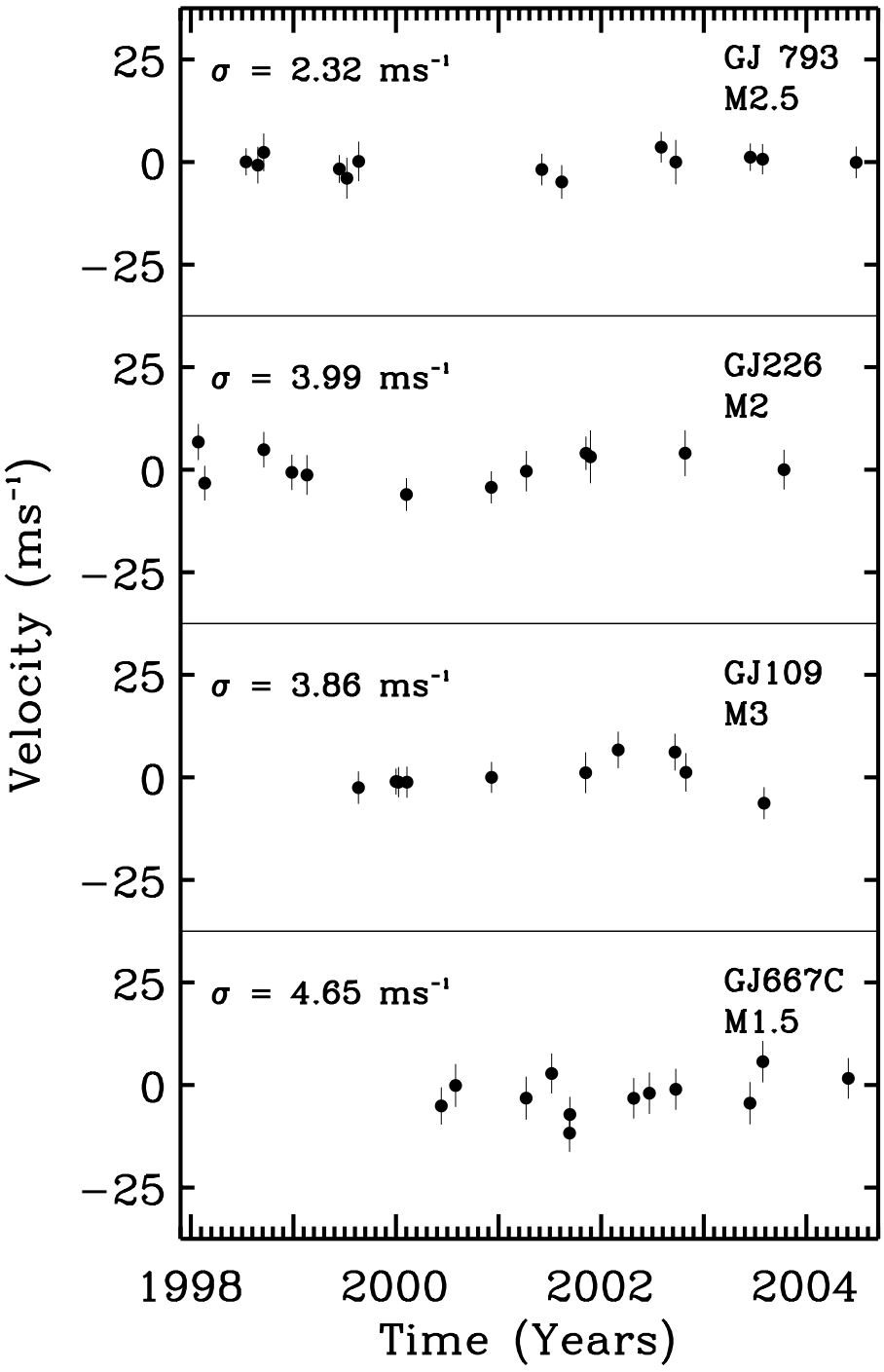

Fig. 2.— Radial velocities vs. time of the comparison M dwarfs shown in Figure 1. These M dwarfs are representative of the middle–aged M1.5 – M3 dwarfs on the program. These stars have 10+ observations over 4+ years. The observed RMS velocity scatter of these stars range from 2.32 to 4.65 m s^{-1}, showing the combined velocity errors and photospheric jitter is $\sim$5 m s^{-1} or less, suggesting that GJ 436 will suffer similar errors.

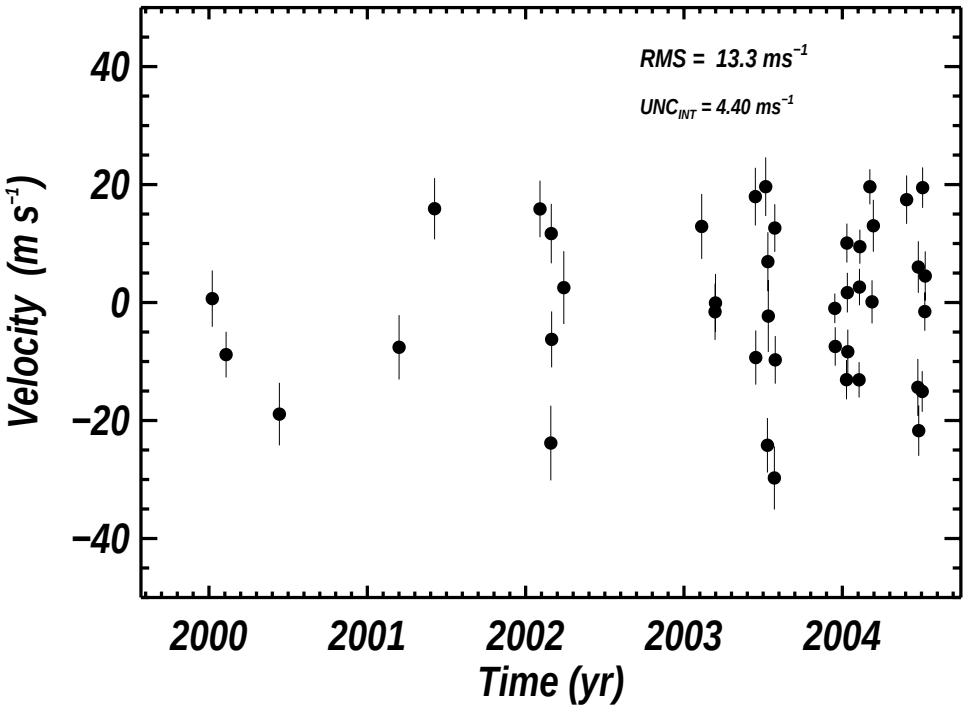

Fig. 3.— Radial velocities vs. time for GJ 436. The observed RMS velocity scatter of 13.3 m s^{-1} is larger than both the median of the internal errors, 4.7 m s^{-1}, and the expected RMS (5 m s^{-1}) revealed by comparison stars (Figure 2). Similarly, the expected photospheric jitter is only 3.3 m s^{-1} . The value of $\sqrt{\chi^2_\nu} = 2.57$, for which the probability of occurrence by chance is less than 0.1%. Thus the velocity scatter in GJ 436 is larger than can be understood by sources of errors and jitter. The velocity zero–point is arbitrary.

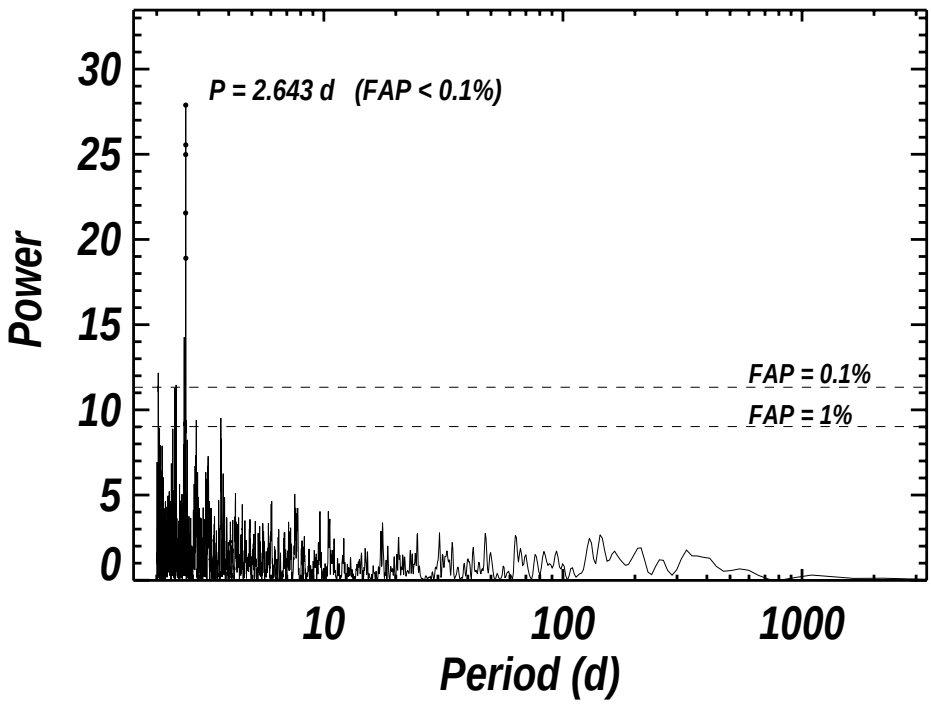

Fig. 4.— The periodogram of the Keck velocities for GJ 436, showing peak power at 2.643 d with a false alarm probability, FAP $< 0.1\%$. The multiple dots near the highest peak show the sampling that resolves the peak. The neighboring peaks are aliases of the 2.64 d period.

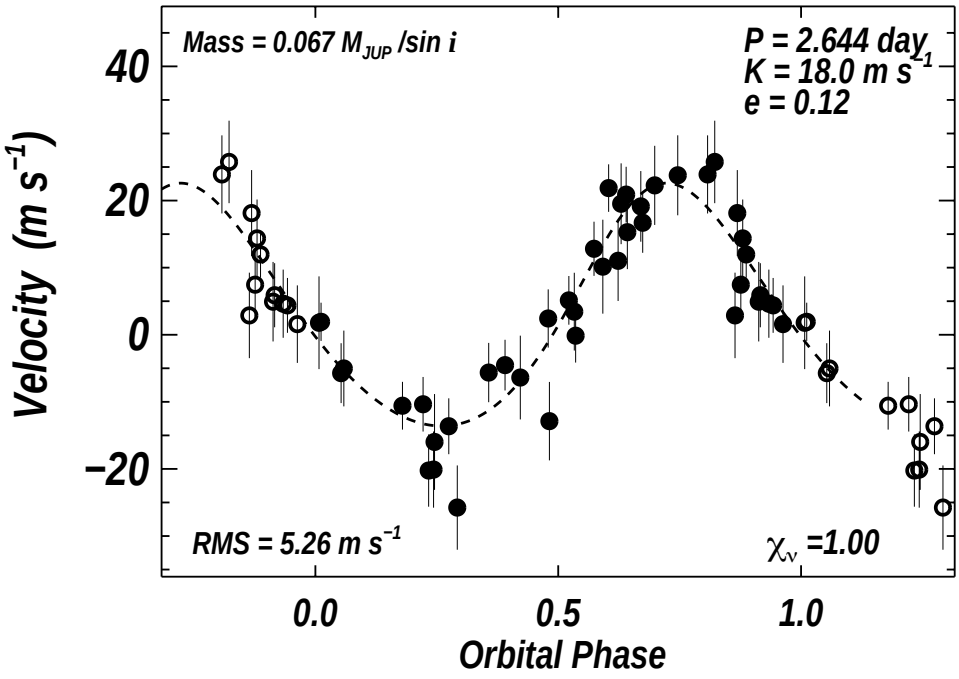

Fig. 5.— Measured velocities vs. orbital phase for GJ 436 (filled dots), with repeated points (outside phases 0–1) shown as open circles. The dotted line is the radial velocity curve from the best–fit orbital solution, $P = 2.644$ d, $e = 0.12$, $M \sin i = 0.067$ $M_{\rm JUP}$. The RMS of the residuals to this fit is 5.26 m s^{-1} with a reduced $\sqrt{\chi^2_\nu} = 1.00$. The error bars show the quadrature sum of the internal errors (median 5.2 m s^{-1}) and jitter (3.3 m s^{-1}). A linear velocity trend is found to be 2.7 m s^{-1} per year.

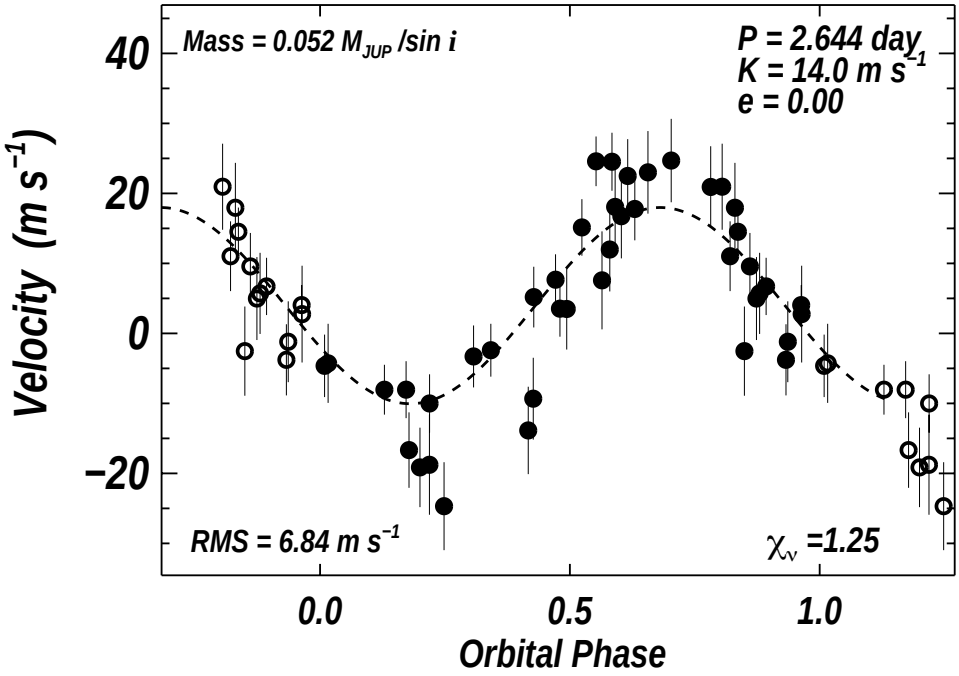

Fig. 6.— Circular orbit fit to GJ 436, overplotted on the measured velocities vs. orbital phase (dots, as in Figure 5). The dotted line represents the sinusoidal fit (circular orbit) and no linear velocity trend, allowing only three free parameters. This orbital fit gives P = 2.644 d, e = 0.0 (forced), K=14.0 m s^{-1}, $M \sin i$ = 0.052 M_{JUP}. The RMS of the residuals is 6.8 m s^{-1} with a reduced $\sqrt{\chi^2_\nu}$ = 1.25, indicating a somewhat poorer fit than for a full Keplerian fit with a floating eccentricity and linear velocity trend (Fig 5). The weights and error bars reflect the quadrature sum of the internal errors (median 5.2 m s^{-1}) and jitter (3.3 m s^{-1}).

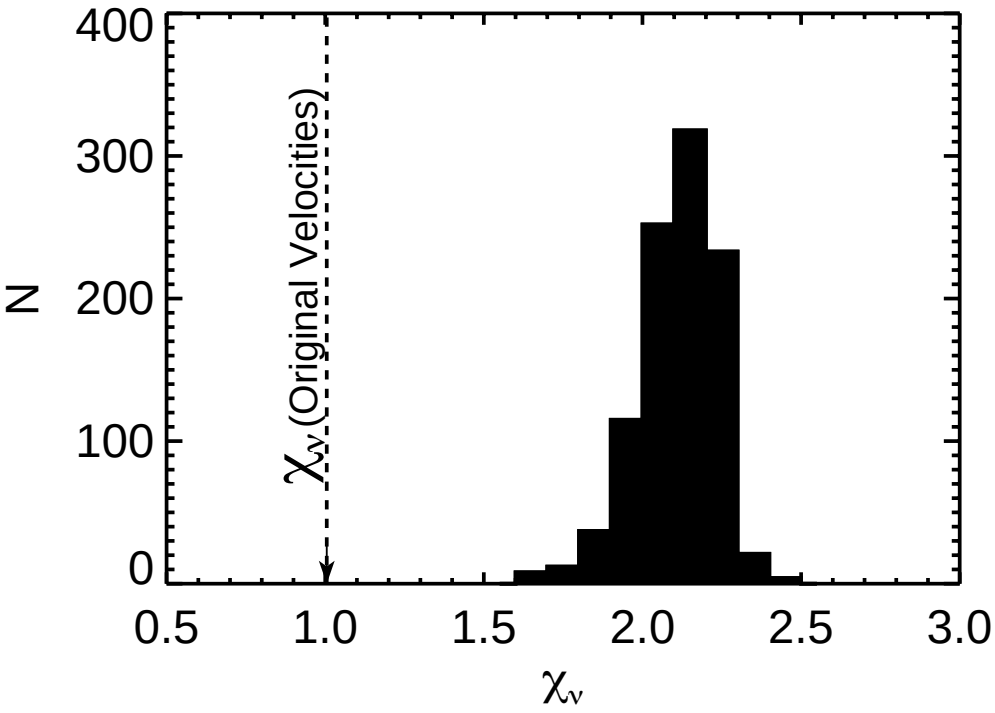

Fig. 7.— Histogram of $\sqrt{\chi^2_\nu}$ from Keplerian fits to 1000 sets of scrambled velocities (filled area). The histogram shows the probability distribution of χ_ν from Keplerian fits that would occur if the velocities were merely uncorrelated noise. The distribution peaks at $\chi_\nu = 2.1$ with a FWHM of 0.3. For comparison, the best–fit orbit to the original velocities gives $\sqrt{\chi^2_\nu}$ = 1.00 (vertical dashed line), which is lower than all 1000 trials. The FAP is apparently much less than 0.1%, in agreement with the F–test that yields FAP $< 0.1\%$.

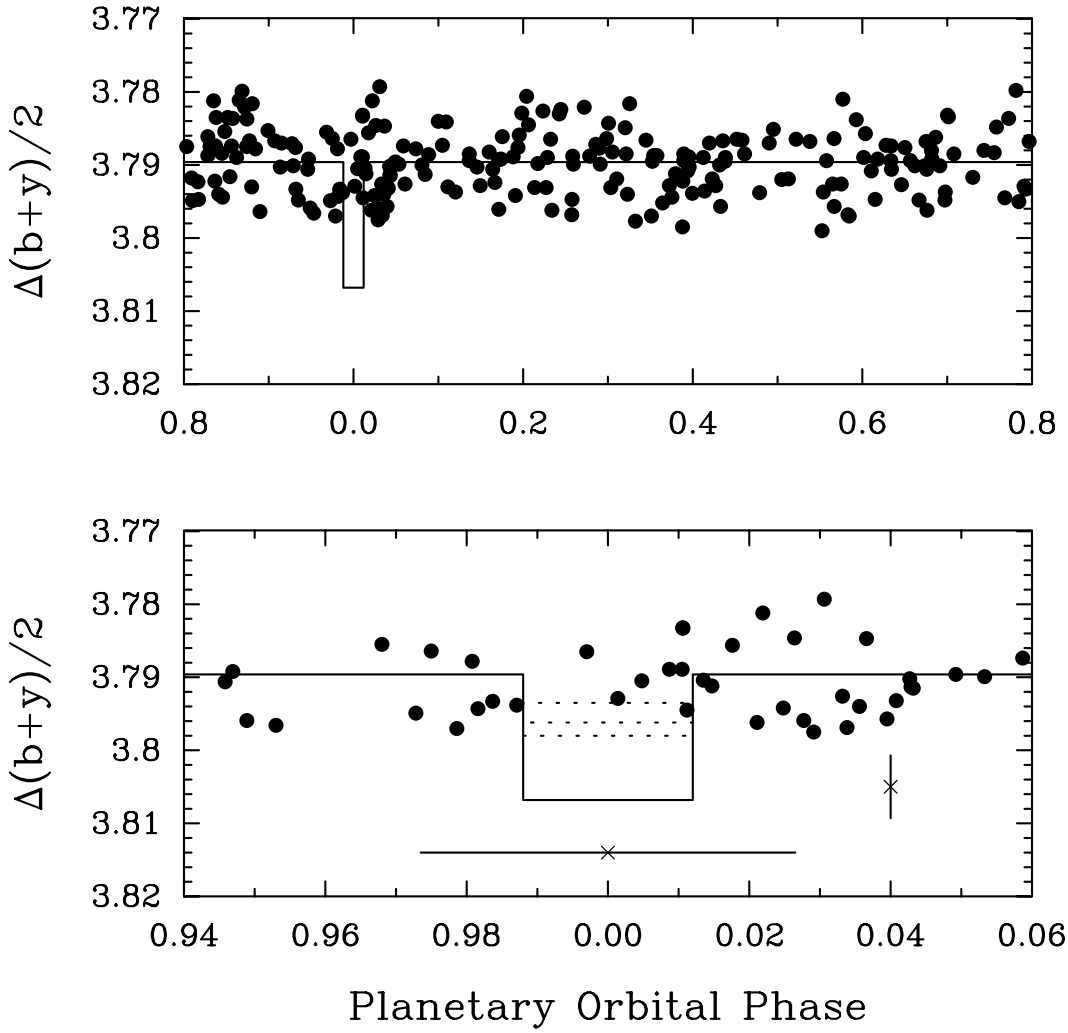

Fig. 8.— Strömgren $(b + y)/2$ photometric observations of GJ 436 acquired with the T12 0.8 m APT at Fairborn Observatory phased to the Doppler perioditiy of 2.644 days (*top*). In particular, the star is constant on the radial velocity period to a limit of 0.0004 mag or better, supporting the planetary interpretation of the radial velocity variations. Predicted transit depths are shown (*bottom*) for various planetary compositions (see text), but are ruled out by the observations.

Table 1. Radial Velocities for GJ 436

JD -2440000	RV (m s^{-1})	Unc. (m s^{-1})
11552.077	0.66	4.8
11583.948	-8.83	3.9
11706.865	-18.91	5.3
11983.015	-7.59	5.5
12064.871	15.90	5.2
12308.084	15.87	4.8
12333.038	-23.82	6.3
12334.054	11.69	5.0
12334.935	-6.25	4.7
12363.039	2.53	6.2
12681.057	12.90	5.5
12711.898	-1.56	4.8
12712.902	-0.07	4.9
12804.878	17.96	4.9
12805.829	-9.33	4.6
12828.800	19.64	5.0
12832.758	-24.20	4.6
12833.763	6.93	5.0
12834.779	-2.30	6.1
12848.752	-29.74	5.3
12849.762	12.63	4.0
12850.763	-9.72	4.0
12988.146	-0.99	2.5
12989.146	-7.45	3.3
13015.142	-13.08	3.3
13016.072	10.08	3.3
13017.046	1.68	3.4
13018.142	-8.34	3.8
13044.113	-13.10	3.0
13045.018	2.62	3.1
13045.984	9.47	2.9
13069.032	19.63	3.0
13073.992	0.12	3.7
13077.066	13.02	4.4
13153.817	17.44	4.1

Table 1—Continued

JD -2440000	RV (m s^{-1})	Unc. (m s^{-1})
13179.759	-14.38	4.8
13180.803	6.02	4.4
13181.746	-21.72	4.3
13189.787	-15.07	3.4
13190.754	19.48	3.4
13195.767	-1.53	3.3
13196.772	4.50	4.2

Table 2. Orbital Parameters for GJ 436

Parameter	
P (d)	2.6441 (0.0005)
T_p (JD)	2451551.507 (0.03)
e	0.12 (0.06)
ω (deg)	332 (11)
K_1 (m s^{-1})	18.10 (1.2)
f_1(m) ($M_\odot$)	1.58e-12
$a_{\rm rel}$(AU)	0.0278
$M \sin i$ (M_{Jup})	0.067 (0.007)
dv/dt (m s^{-1} per yr)	2.7
Nobs	42
RMS (m s^{-1})	5.26
$\sqrt{\chi^2_\nu}$	1.00